Conference Paper, Published Version

Jongeling, T. H. G.; Jagers, H. R. A.; Stolker, C.

Design of granular bed protections using a RANS 3Dflow model

Design of granular bed protections using a RANS 3D-flow model

T.H.G. Jongeling*, dr. H.R.A. Jagers*, and C. Stolker*
* WL | Delft Hydraulics, Delft, The Netherlands

This paper presents a numerical method that can be used to design the top layer of a granular bed protection near hydraulic structures. On the basis of the computed flow pattern and turbulence level both the required weight of the stones (the strength) and the extent of the protection can be determined.

I. INTRODUCTION

In the framework of a basic-research project [Ref. 1] the authors have studied the possibilities to design a granular bed protection applying the results of a numerical flow computation. Starting point for our research was that a RANS code with standard turbulence model should be used.

Experiments were carried out in a scale model for different geometries and flow conditions, including flow over a flat horizontal bed, flow over a flat bed with a transverse slope, different sill configurations with overflow, and flow through openings in a vertical plate. In all cases the bed was protected with stones and the flow conditions were such that individual stones were now and than moved by the flow ('incipient motion' condition). In this situation flow patterns, flow velocity profiles and turbulence profiles were measured.

Next, these experiments were simulated in the numerical flow model and the results of experiments and simulations mutually compared. A flow force quantity, composed of computed flow velocity and turbulence level, was such defined that it represents the dynamic load on the top layer of the protection. The flow force quantity was computed in the entire flow field and averaged over a representative part of the water body above the bed, thus taking into account relevant flow and turbulence phenomena.

Finally, we have established a new stability parameter similar as the well-known Shields parameter, that relates the flow force quantity to the strength of the granular bed protection. The value of this stability parameter at incipient motion of the stones ('critical value') was derived from our experiments. The critical value of the parameter is in principle independent of the considered geometry and bed layout.

With the help of the developed numerical method a designer can compute the required weight of the stones of the top layer (expressed in terms of the nominal stone diameter) and decide on the extent of the protection.

The new method has been applied to a fictitious case of a sluice in a dike, that discharges surplus water into the sea. The bed protection at the downstream side of the sluice was computed and compared with the results of an analytical design method.

In next sections we will explain the numerical design method more into detail.

II. EXPERIMENTS IN A SCALE MODEL

Experiments in a scale model were executed in a 0.5 m wide, glass-walled flume with effective length of 23 m. The water in this flume wais circulated by means of a pump in a return conduit underneath the flume.

The considered geometries inclusive the stone-protected bed, were constructed after a distance of about 14 m from the inflow. The entire bottom of the flume in the approach section to the model was covered with a fixed layer of stones, with mean diameter of 7.4 mm (nominal stone diameter D_n = 6.2 mm). At the location of the model similar, loosely packed stones were applied in a 40 mm thick layer. These stones were laid down in bands with different colors, which enabled the observation and counting of moving stones. Fig. 1 presents an overview of the various modeled geometries.

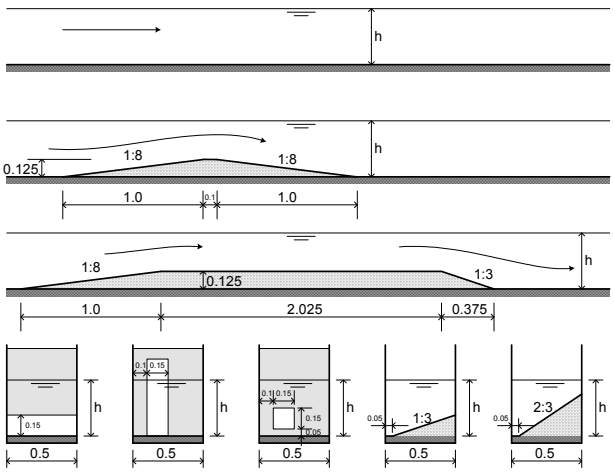

Figure 1. Experiments in scale model: overview of modeled geometries (flat bed, short-crested sill, broad-crested sill, underflow gate, plate with vertical slit, plate with square opening, transverse slope 1:3, transverse slope 2:3)

The initial geometry consisted of a flat horizontal bed without any structure. Than a short-crested sill with upstream slope 1:8, downstream slope 1:8, and height of 125 mm was modeled, followed by a broad-crested sill with upstream slope 1:8, steep downstream slope 1:3, height of 125 mm and crest width of 2.0 m. Next, a

vertical plate was fit in the flume with the lower edge at 150 mm above the stone protected bed ('underflow gate'). A second plate had an eccentrically, 150 mm wide, vertical slit, and a third plate was provided with an eccentrically, square opening, with sides of 150 mm and lower edge 50 mm above the bed. All edges of the openings in the plates were beveled, with the sharp angle at the downstream side. Finally, also a flat bed with a transverse slope 1:3 and 2:3 successively was modeled.

The flow conditions during the tests were such that individual stones of the bed protection were occasionally moved and transported by the flow. This 'incipient motion' flow condition was found by a stepwise increasing of the flow velocity in the flume and counting the number of displaced stones as a function of the flow velocity. The quantity of displaced stones per unit of time was chosen as a measure to assess the flow conditions that are representative for incipient motion.

Vertical flow velocity profiles were measured in the centre line of the flume and in lines parallel to the centre line. The three flow velocity components u, v and w along a Cartesian x, y and z coordinate system (x in longitudinal direction of flume, z in vertical direction) were measured using a Laser Doppler anemometer (u and w components) and an electro-magnetic flow meter (u and v components). The mean values $\overline{u}$, $\overline{v}$ and $\overline{w}$ were used to analyze flow patterns, while the standard deviations σ_u, σ_v and σ_w, which were combined in the quantity

$$k = 0.5*(\sigma_u^{\,2} + \sigma_v^{\,2} + \sigma_w^{\,2}) = a.\sigma_u^{\,2} \qquad (1)$$

, were used to compute turbulence intensity profiles. An example of the measured flow velocity and turbulence intensity profiles is shown in Fig. 2a/b for the case of flow over a broad-crested sill.

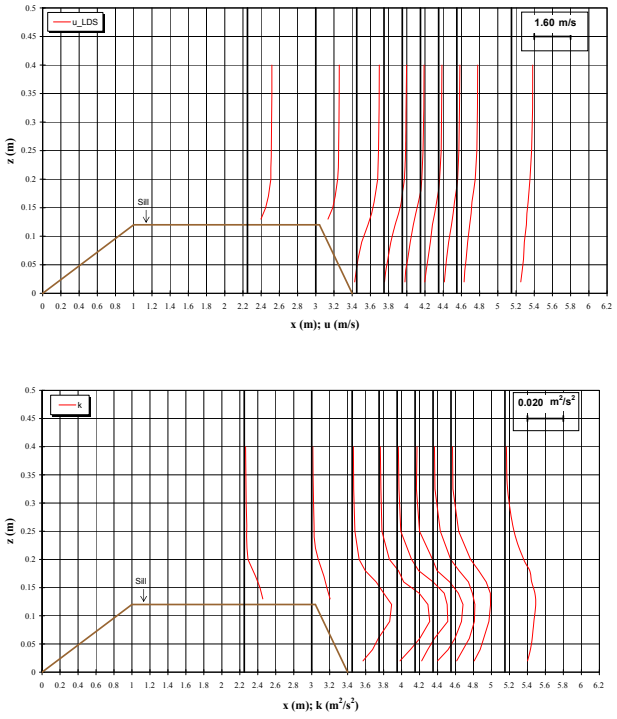

Figure 2. Experiment: flow over broad-crested sill, water depth 0.5 m; top (a): horizontal flow velocity u, bottom (b): turbulence intensity k; center line of flume

Fig. 3 gives an impression of the flow through a square opening in a vertical plate, that expands above the granular bed.

Figure 3. Experiment: flow through square opening in a vertical plate; the jet expands above the granular bed

It is interesting to note that, in the case of a fully developed flow over the stone-protected flat horizontal bed, σ_u in the zone near the bed was about a factor 2.2 as high as σ_v and σ_w, while the ratios σ_u / σ_v and σ_u / σ_w reduced to about 1.3 towards the water surface. When we assume a ratio of 2.2 in the region above the bed, the application of Equation (1) leads to a value a = 0.7. Towards the water surface the factor a increases to 1.1. In the case of jet flows through openings in the vertical plate the ratios of these standard deviations were almost equal to 1.0 in the core of the jet (a ≈ 1.5), but outside the jet, in the turbulent region, the σ_u component was strongly dominant compared to the σ_v and σ_w components (ratio between 1.5 and 2.0).

III. NUMERICAL SIMULATIONS

The experiments in the flume have been simulated using the RANS code CFX, version 4.4. This code has different turbulence models, among others the standard k-ε model and the RNG k-ε model. Both turbulence models have been applied in the simulations. With the parameters k (turbulent kinetic energy) and ε (dissipation of turbulent energy) the development and decay of the turbulence of the flow is described. Both the flow velocity and the turbulence level, which vary throughout the flow field, are used in our design method.

Lift and drag forces acting on individual stones of the protection are related to the local flow velocity; force fluctuations are related to perturbations in the flow field above the bed. In particular vortices with dimensions greater than the stone diameter (characteristic size ranging from the stone diameter up to the water depth) are relevant. Since the dynamic component of the flow force contributes to a large extent to the destabilizing load on the stones, it is of utmost importance that the turbulence quantity k of the numerical model adequately represents the turbulent nature of the flow in space and time. Much attention was therefore paid to compare the quantity k of the numerical model with the quantity k as defined with Equation (1). Especially, those regions of the flow where significant turbulence is generated such as the region near the rough, stone-protected bed and the free shear layer region near jet flows and in wakes behind structures were mutually compared.

The mesh of the numerical model was built up as a structured grid, with a refinement in regions where steep velocity gradients occur (near walls, flow openings, stone-

protected bed). Geometries with uniform properties in transverse direction of the flume (flat bed, sills, underflow gate) were modeled as a quasi 2DV grid with symmetry boundary conditions at the sides. This simplification implied that transverse flow phenomena, if any, were neglected and not simulated.

The free water surface was either modeled as a rigid lid with free-slip condition or as a moving water surface with adaptation of the thickness of the top layers of the grid. Attention was also paid to a correct modeling of the roughness of the stone-protected bed in the numerical model. From a comparison of experiments and simulations it appeared that with a roughness height corresponding to $2.D_n$ (D_n = nominal stone diameter) the best results in terms of flow velocity and turbulence gradients were obtained. This roughness height was selected in further simulations.

The comparison of experiments and simulations led to the next conclusions:

- Uniform flow over a flat, stone-protected bed. The flow is well computed when the k-ε model is applied; velocity profiles and turbulence profiles (k) show a satisfactorily similarity with measured profiles. The turbulence levels are at the high side when the RNG k-ε model is applied.
- Flow over a stone-protected short-crested sill with mild slopes 1:8; flow over a broad-crested sill with steep downstream slope 1:3. In the case of a mild downstream slope the flow remains attached, while in the case of the steep slope the flow detaches from the crest and remains detached. These flow patterns are in general correctly simulated. When the k-ε model is applied flow velocity and turbulence profiles above the downstream slope and downstream bed are reasonably well computed. With the RNG k-ε model flow patterns are well computed but the turbulence level at the downstream side of the sill is somewhat too low. Some results for flow over the short-crested and broad-crested sill are shown in Fig. 4a/b and Fig 5a/b.
- Flow through openings in a plate with stone-protected bottom at upstream and downstream side (underflow gate, vertical slit, square opening). Generally, the development of jet flows and attachment at flume walls and bottom is reasonably well predicted, but when the k-ε model is applied the jet flow widens faster in the simulation than in the experiments. In addition, the turbulence level in the free shear layer region is too high, in particular near the outflow opening in the plate. Better results are obtained when the RNG k-ε model is applied: the widening of the jet is better predicted, but as a consequence the turbulence level is somewhat too low. Fig. 6a/b present some results for the flow through a slit in a vertical plate.
- Flow over a flat, stone-protected bed with transverse slope. Similar as for a horizontal bed the flow is well computed, but with the RNG k-ε model turbulence levels are at the high side.

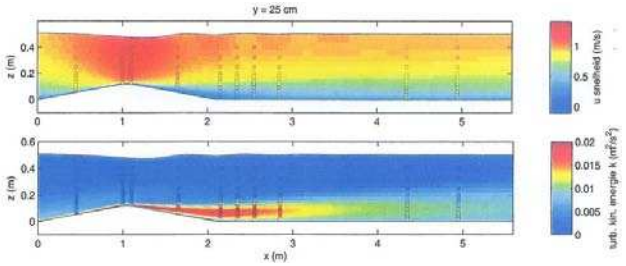

Figure 4. Simulation: flow over short-crested sill, water depth 0.5 m; top (a): horizontal flow velocity u, bottom (b): turbulence intensity k; vertical center-line plane; RNG k-ε turbulence model

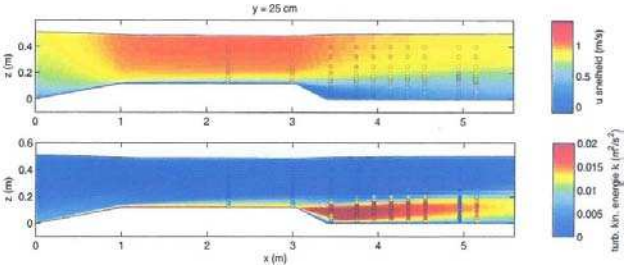

Figure 5. Simulation: flow over broad-crested sill, water depth 0.5 m; top (a): horizontal flow velocity u, bottom (b): turbulence intensity k; vertical center-line plane; RNG k-ε turbulence model

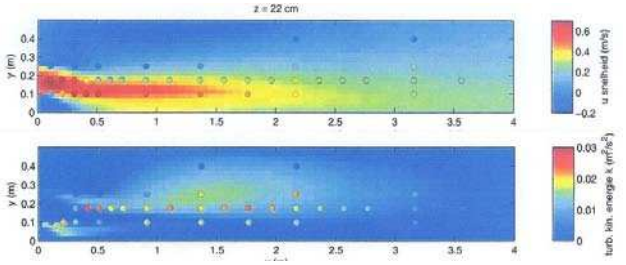

Figure 6. Simulation: flow through slit in vertical plate, water depth 0.5 m; top (a): horizontal flow velocity u, bottom (b): turbulence intensity k; horizontal plane at 0..22 m above bed; RNG k-ε turbulence model

The properties of the turbulence model influence the flow velocity profiles and turbulence distribution. The RNG k-ε model predicts better the gradual widening of jets, but the corresponding turbulence level of the free shear layer region is somewhat too low. The standard k-ε model produces satisfactorily results for flow over a flat, stone-protected bed as well as the RNG k-ε model, but the latter model overestimates the turbulence level. Since a correct simulation of the flow pattern is important in the numerical design of a granular bed protection we will use the results of simulations with the RNG k-ε model in next analysis. The effect of turbulence is accounted for through a combination of the turbulent kinetic energy k and a turbulence magnification factor α. The factor α can also be used to improve the computed turbulence level.

We have not studied flow situations where local, strong energy dissipating effects occur (such as the energy loss in a hydraulic jump).

IV. DEFINITION OF FLOW FORCE QUANTITY AND STABILITY PARAMETER

It is common practice in an analytical approach to describe the flow forces that are acting on the bed protection in terms of flow velocity and turbulence intensity. The required strength of the granular protection is assessed using a stability predictor, for example the well-known

Shields parameter Ψ. This parameter relates the flow force and the strength; the classical relationship for uniform flow over a flat bed reads:

$$\Psi = \frac{\overline{\tau}_b}{\rho g \Delta D_n} = \frac{\overline{u}_*^{\,2}}{g \Delta D_n} = \frac{\overline{U}^2}{C^2 \Delta D_n} \qquad (2)$$

where:

τ_b	= bed shear force
Δ	= relative density = $(\rho_{stone} - \rho) / \rho$
ρ	= density of water
g	= gravitational acceleration
D_n	= nominal stone diameter
u_*	= bed shear velocity
C	= Chézy coefficient related to the roughness of the stones
U	= flow velocity

Time-averaged quantities in the formula are indicated with a horizontal bar. The Shields parameter is a function of the Reynolds number (Re = $u_*.D_n/\nu$). For Reynolds numbers greater than about 600 the Shields parameter tends to a constant value; in practice this corresponds to a flow over a bed with particles greater than about 5–10 mm diameter. The value of the Shields parameter depends on the transport condition: a value of 0.032 is usually selected for incipient motion of stones. Particular geometrical, flow and turbulence phenomena are included in the analytical approach by multiplication of the flow velocity $\overline{U}$ with empirical coefficients.

In a numerical approach the effect of the geometry is already included in the flow computation and it is convenient to express the quasi-static and dynamic components of the flow force in terms of flow velocity U and turbulent kinetic energy k only. Since it is not feasible to simulate the dynamic flow force on each individual stone of the bed protection, we define the flow force as a generalized, global force per unit of area of protected bed. This force varies as a function of space.

A granular bed protection is generally designed to remain stable under the action of the hydraulic loads which occur during the anticipated lifetime of the protection, inclusive extreme loads with small probability. The flow force is roughly proportional to the velocity squared and fluctuates as a function of time. Small and large scale turbulence contributes to the flow force in a more or less chaotic way, but in particular the low-frequency part of the turbulence, corresponding to vortices with dimensions of the same order of magnitude as the stone diameter or larger, leads to a significant fluctuation of the flow force. From experimental research [Ref. 2] it is known that individual stones of the top layer become unstable and are moved when strong vortices pass.

The flow velocity can be expressed as:

$$U(t) = \overline{U} + U'(t) \qquad (3)$$

where $\overline{U}$ = local, time-averaged component and $U'(t)$ = fluctuating component. In the numerical approach with the RANS model the mean flow component $\overline{U}$ is computed, but not the fluctuating component $U'(t)$; instead the turbulent kinetic energy k, a scalar quantity, is computed. This quantity represents the mean dynamic character of the flow, and is selected in our numerical approach as base variable, together with the mean velocity $\overline{U}$. To account for peak values that occur in the real flow we define:

$$U_{peak} = \overline{U} + \alpha.\sqrt{k} \qquad (4)$$

whereas the flow force on the bed related to this peak flow is assumed to be proportional to:

$$\rho.\left(\overline{U} + \alpha.\sqrt{k}\right)_d^{\,2} \qquad (5)$$

The coefficient α in this generalized flow force quantity can be regarded as a turbulence magnification factor. The subscript d denotes that the flow force quantity is averaged in a representative region above the bed.

The relationship between the generalized flow force quantity based on the numerical variables $\overline{U}$ and k, and the strength of the bed protection is defined with the help of a new, dimensionless stability parameter Ψ_{u-k}, similar as the Shields parameter:

$$\Psi_{u-k} = \frac{\rho.\left(\overline{U} + \alpha\sqrt{k}\right)_d^{\,2}}{\rho g \Delta D_n} \qquad (6)$$

For design purposes we rewrite this expression as:

$$D_n \geq \frac{\left(\overline{U} + \alpha\sqrt{k}\right)_d^{\,2}}{g\Delta.\left(\Psi_{u-k}\right)_{crit}} \qquad (7)$$

The value of $(\Psi_{u-k})_{crit}$ corresponds to incipient motion of the stones. For a fully stable bed protection a smaller value than $(\Psi_{u-k})_{crit}$ may be selected or a safety factor applied to the design flow velocity.

V. CRITICAL VALUE OF STABILITY PARAMETER

The stability parameter Ψ_{u-k} relates the generalized flow force on the bed protection to the 'under-water weight' of the stones. The critical value $(\Psi_{u-k})_{crit}$ marks the flow condition with incipient motion of stones; this critical value is in principle independent of flow pattern and bed layout, provided that all relevant phenomena are included in either the generalized flow force quantity or the under-water weight of the stones. This is however, generally not the case and one may expect that a certain range of values is obtained for $(\Psi_{u-k})_{crit}$ when experiments and computations are done for bed protections with different layout and flow conditions, depending also on the criterion that is used to define the transport condition of the stones. Similar as the Shields parameter Ψ the stability parameter Ψ_{u-k} is a function of the Reynolds number. The dependency fades above a Reynolds number of about 600, which in practice is applicable to almost all design cases.

In our study we have concentrated on the value of the stability parameter Ψ_{u-k} at incipient motion of the stones. The value of Ψ_{u-k} as a function of space was computed from the location-depending variables $\overline{U}$ and k of the

numerical simulations (the RNG k-ε turbulence model was applied). To get insight in the sensitivity of the generalized flow force quantity $\rho.\left(\bar{U}+\alpha.\sqrt{k}\right)_d^2$ to a variation of the fluid control volume above the bed and the turbulence level, we have systematically varied the averaging depth d and the turbulence magnification factor α. From the analysis it appeared that the turbulence factor α is generally a much more important factor than the averaging depth d. The latter was eventually selected as:

$$d = 5D_n + 0.2h \le h \qquad (8)$$

where h = local water depth, and d = thickness of water layer directly above the bed.

The selection of d as a combination of stone diameter D_n and a fraction of the local water depth h followed from the practical consideration that the flow velocity and the turbulence level in the region near to the bed are particularly of importance for the stone stability. The turbulence level in the RANS model is related to flow gradients, which are highest near the bed or near free shear layers. In general it is true: the rougher the bed (modeled as $2.D_n$ in the simulations), the more turbulent kinetic energy is produced and the thicker the layer above the bed with an increased turbulence level. With the sum $5D_n + 0.2h$ we have in a pragmatic way accounted for the effects of stone diameter and increased turbulence level. We appreciate that other averaging depths or weighing functions for the flow force quantity may also be defined, but in RANS models the effect of other choices is expectantly only small.

In the analysis we have searched for combinations of α and d where at incipient motion of stones the stability parameter $\Psi_{u\text{-}k}$ had more or less an equal value for all considered geometries. An example of this analysis is shown in Fig. 7a/b/c. These figures present the value of the parameter $\Psi_{u\text{-}k}$ as a function of x and y at the downstream side of a plate with a vertical slit. The averaging depth d is selected as $5.D_n + 0.2h$ and the computed $\Psi_{u\text{-}k}$ -values are shown for α = 3, 6 and 10 respectively.

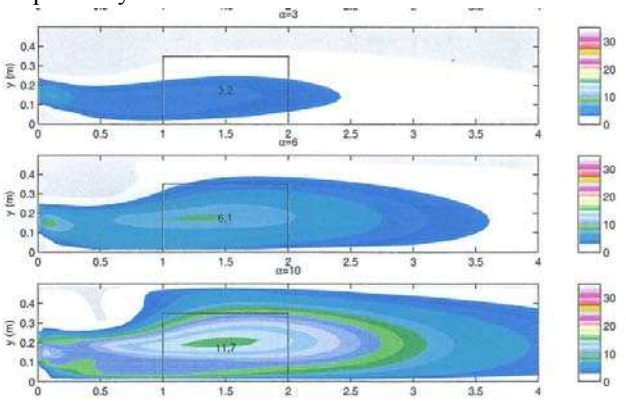

Figure 7. Simulation: flow through slit in vertical plate, water depth 0.5 m; stability parameter $(\Psi_{u\text{-}k})_{crit}$; top (a): α = 3, middle (b) α = 6, bottom (c): α = 10; rectangles indicate areas with damage in experiment; RNG k-ε turbulence model

The rectangle in the plots indicates the location where transport of stones occurred in the corresponding scale model test; the number in the rectangle corresponds to the $\Psi_{u\text{-}k}$ –value of that location.

After a mutual comparison of the various geometries it appeared that the variation of the stability parameter $\Psi_{u\text{-}k}$ is smallest when a value α = 6 is selected. This relatively high value of the turbulence magnification factor is an appropriate value considering that at the incipient motion flow condition individual stones are only moved as a result of incidental, strong flow and turbulence events. Expressed in terms of the standard deviation σ_u of the main flow component u we find with Equation (1) and k = a*σ_u^2 = 0.7*σ_u^2 for the case of uniform flow over a flat bed:

$$u + \alpha\sqrt{k} = u + \alpha\sqrt{0.7*\sigma_u^2} = u + 5.\sigma_u \qquad (9)$$

when a turbulence factor α = 6 is applied. This result indeed expresses that only the strongest flow variations are responsible for the incidental transport of stones at the incipient motion flow condition.

Application of the RNG k-ε turbulence model in combination with α = 6 and $d = 5D_n + 0.2h$ revealed critical values for the stability parameter $\Psi_{u\text{-}k}$ in the range 9 – 14, with a mean value of 12.0. An exception appeared to be the situation with flow over a transverse slope 1:3; in this situation a value $(\Psi_{u\text{-}k})_{crit}$ = 17.5 was found (notice that the steeper transverse slope 2:3 revealed a value $(\Psi_{u\text{-}k})_{crit}$ = 11.8).

For design purposes we recommend that a safe value $(\Psi_{u\text{-}k})_{crit}$ = 8.0 is used (in combination with the RNG k-ε turbulence model, α = 6 and $d = 5D_n + 0.2h$). When more data has become available and experience with the new method has been built up a more economic, somewhat higher value for $(\Psi_{u\text{-}k})_{crit}$ may be selected.

VI. CASE STUDY

The new design method has been applied to the case of a discharge sluice. This sluice spills surplus storm water from a lake into the sea. The sluice consists of five gated flow openings, see Fig. 8, each opening having a width of 33 m between the piers. The horizontal floor at a level of 6.5 m below NAP (= datum) has a downward step at the downstream side of the sluice, see Fig. 9. The design flow velocity amounts to 6.7 m/s between the piers (gates fully lifted above the water surface); this velocity corresponds to a design discharge of 1060 m^3/s per flow opening. Two breakwaters which protrude into the sea, shield the sluice from the incoming waves.

The bed at the sea side of the sluice is protected with stones. The required stone diameter was preliminary estimated using Shields stability parameter. The estimated flow velocity $\bar{U}$ was multiplied by a specific turbulence amplification factor. This resulted in a stone grading of 300 – 1000 kg, 60 – 300 kg and 10 – 60 kg, laid down in successive bands behind the 40 m wide concrete slab at the downstream side of the sluice.

A full three-dimensional model was set up that covered three adjacent flow openings, including the left side opening. A simulation was done for design flow conditions using the RNG k-ε turbulence model; the computed flow pattern in a horizontal plane at a level of 2 m below datum is shown in Fig. 10.

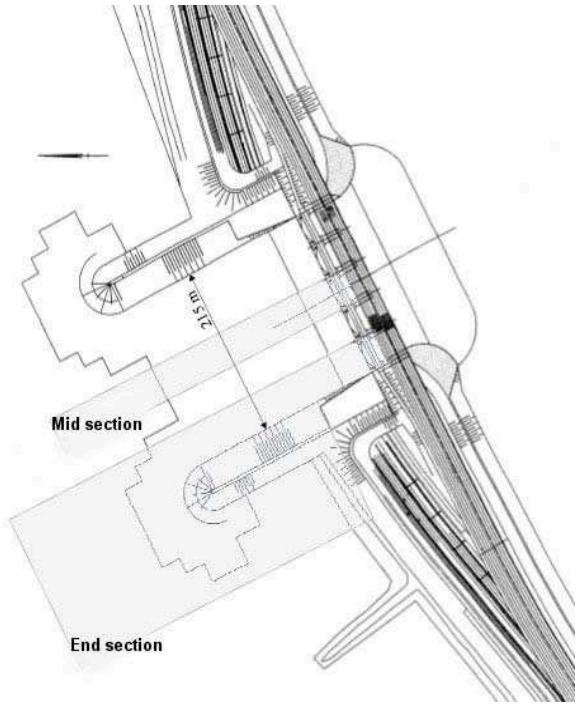

Figure 8. Case study: bed protection downstream of sluice; situation of sluice with indication of applied sub-models

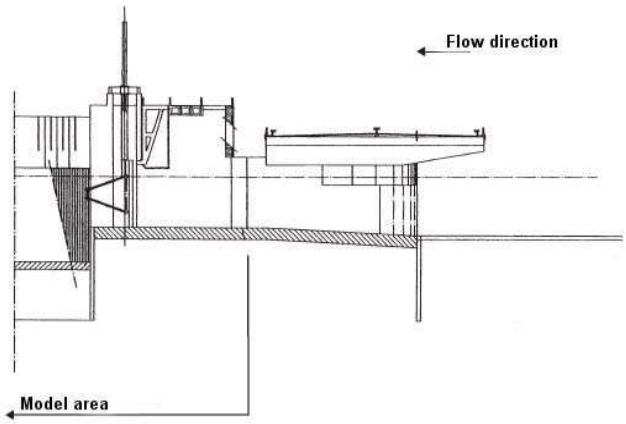

Figure 9. Case study: bed protection downstream of sluice; vertical section of sluice

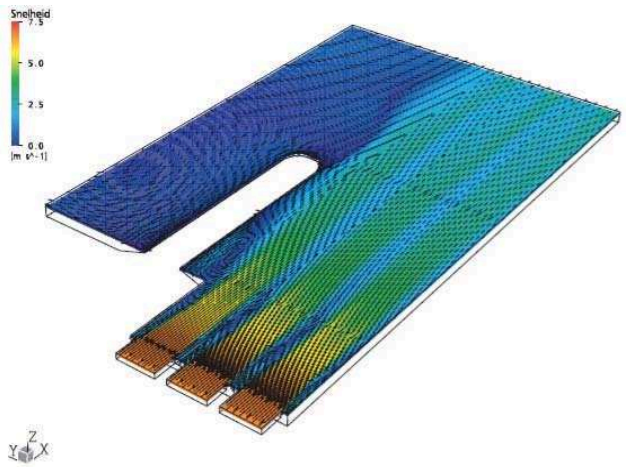

Figure 10. Case study: bed protection downstream of sluice; model of three flow openings; computed flow pattern in plane z = -2 m

From this simulation we could conclude that the flow pattern is symmetrical about a longitudinal axis through a pier between two adjacent flow openings. This enabled the set up of sub-models for individual flow openings only, using symmetry boundary conditions along the sides. One sub-model was built for the central flow opening, one sub-model for the left flow opening (see Fig. 8).

We started with the central opening and modeled the roughness of the bed as $2.D_{n50}$, with D_{n50} corresponding to the mean nominal diameter of the preliminary estimated stone grading. The computed horizontal flow component u, the turbulent kinetic energy k and flow vectors in a vertical longitudinal plane are shown in Fig. 11a/b/c. As can be seen, high turbulence levels are computed in the region of the free shear layer, immediately downstream of the downward step in the floor. The jet widens and attaches to the bed, and simultaneously the turbulent kinetic energy k spreads over the water depth and dampens; eventually the turbulence level adapts to the local bed roughness. The widening of the flow occurs also in a transverse horizontal direction.

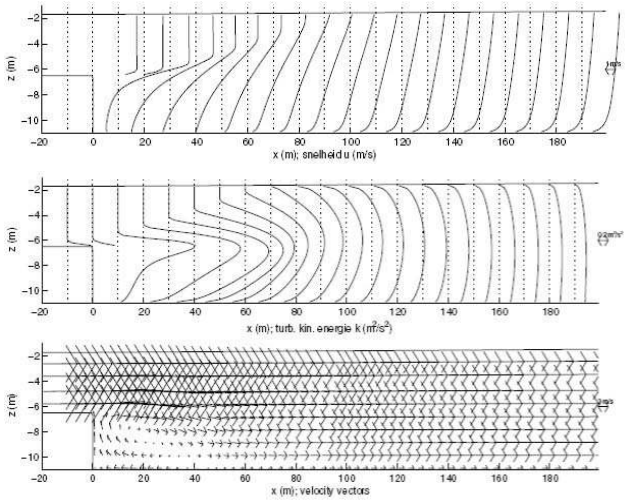

Figure 11. Case study: bed protection downstream of sluice; model of central flow opening; top (a): horizontal flow velocity u, center (b): turbulence intensity k, bottom (c): velocity vectors

Using Equation (7) and the location-dependent variables $\bar{U}$ and k, and selecting the values $(\Psi_{u\text{-}k})_{crit} = 8.0$, $\alpha = 6$ and $d = 5D_n + 0.2h$, we have computed the required mean stone diameter D_{n50} of the protection at the downstream side of the sluice. The results are shown in Fig. 12a/b/c; (a): computed stone diameter, (b): first-estimated stone diameter that was used to model the bed roughness, (c): comparison between computed and first-estimated stone diameter in the central axis of the model. The comparison shows that the difference between first-estimated stone diameter and computed stone diameter is already small. In the next iteration-step we have used the computed stone diameter to improve the bed roughness of the model. The results of the second simulation are shown in Fig. 13a/b/c; (a): computed stone diameter, (b): first-iteration stone diameter that was used to improve the bed roughness, (c): comparison between computed stone diameter and first-iteration stone diameter in the axis of the model. Fig. 13c demonstrates that the computed stone diameter is only slightly different compared to the stone diameter of the first iteration. It appears also that the stone

diameter decreases continuously from the slab behind the sluice to the downstream side of the model. With these computational results a designer is now able to define the extent of the area that has to be protected, and to select the stone grading that corresponds best with the computed stone diameter.

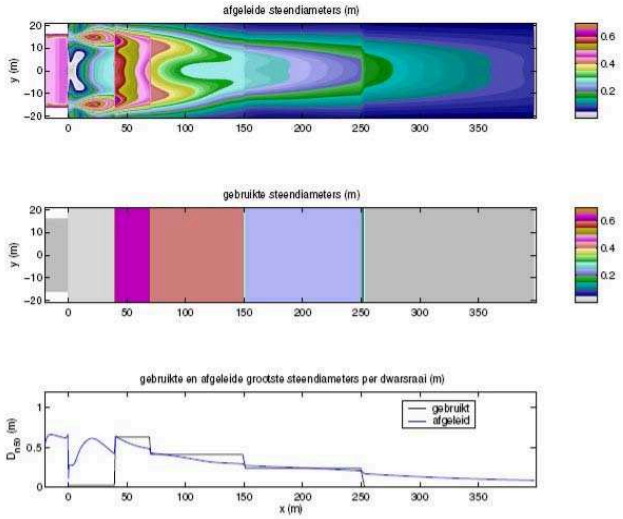

Figure 12. Case study: bed protection downstream of sluice; model of central flow opening; 1st iteration; top (a): computed stone diameter, middle (b): stone diameter used to model the bed roughness, bottom (c): comparison of initial and computed stone diameter, center line of model

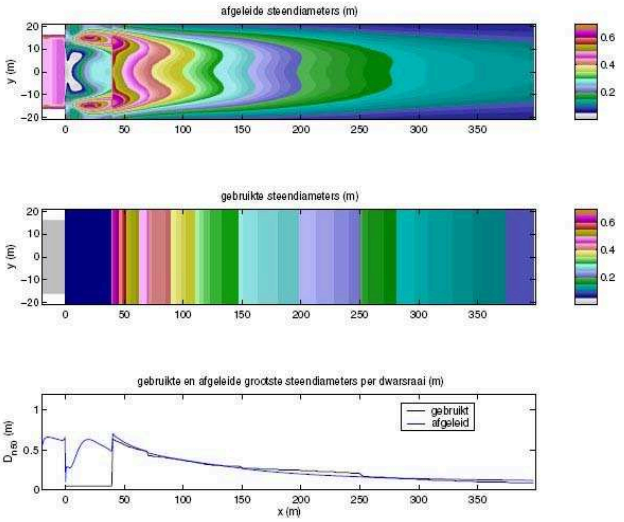

Figure 13. Case study: bed protection downstream of sluice; model of central flow opening; 2nd iteration; top (a): computed stone diameter, middle (b): stone diameter used to model the bed roughness, bottom (c): comparison of initial and computed stone diameter, center line of model

A similar procedure has been used to compute the required stone diameter of the bed protection behind the side opening. The stone diameter of the central opening was used to model the bed roughness. The results of the first simulation run are shown in Fig. 13a/b; (a): computed stone diameter, (b): stone diameter used to model the bed roughness. In a second iteration the stone diameter was only slightly adapted.

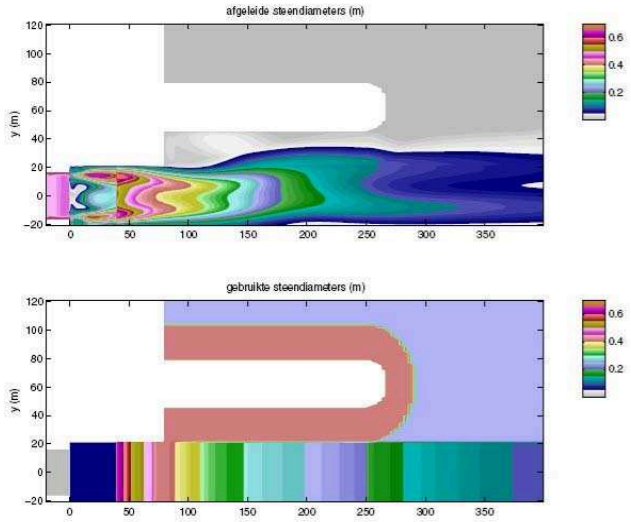

Figure 14. Case study: bed protection downstream of sluice; model of left flow opening; 1st iteration; top (a): computed stone diameter, bottom (b): stone diameter used to model the bed roughness

VII. CONCLUSIONS

A numerical method has been developed for the design of a granular bed protection near hydraulic structures. The method is based on a three-dimensional flow computation applying a RANS code and standard turbulence model. The location-depending variables $\bar{U}$ (time-averaged flow velocity) and k (turbulent kinetic energy) are used to compose a flow force quantity, that represents the dynamic load on the bed protection. A stability parameter relates the flow force to the required stone weight.

The method is found to be reliable as long as the numerical flow model is able to correctly predict the flow pattern, in particular at the downstream side of structures. The latter is, however, not always a trivial matter. Designers therefore should be aware of possible shortcomings of RANS flow models. In any case, insight in the real hydraulic processes is required and a thorough knowledge of modeling techniques. The method has not yet been tested for super-critical flows.

ACKNOWLEDGEMENTS

The Dutch Ministry of Public Works is gratefully acknowledged for their financial support in several stages of the research project.

RFERENCES

[1] WL | Delft Hydraulics; “Ontwerpmethodiek granulaire verdedigingen”, Report Q2933/Q3018, December 2003 (in Dutch)

[2] Hofland, B.; “Rock & Roll; Turbulence-induced damage to granular bed protections”, Thesis Delft University of Technology, December 2005.